JOURNAL OF MATERIALS SCIENCE 32 (1997) 4895–4900

Silicon oxide thin films prepared by a photo-chemical vapour deposition technique

T. JANA, S. GHOSH, S. RAY
Energy Research Unit, Indian Association for the Cultivation of Science, Calcutta - 700 032, India

Wide band gap *a*-SiO_x:H films have been prepared by the photochemical decomposition of a SiH_4, CO_2 and H_2 gas mixture. Deposition parameters namely the CO_2 to SiH_4 gas flow ratio, H_2 dilution and chamber pressure were optimized in order to achieve highly photoconducting (1×10^{-6} S cm^{-1}) films with an optical gap of 1.99 eV. The optical gap was found to increase with an increase in the CO_2 to SiH_4 flow ratio. A decrease in the photoconductivity, refractive index, spin *g*-value and a simultaneous increase in the spin density are attributed to an incorporation of oxygen into the films. Upon hydrogen dilution the photoconductivity of *a*-SiO_x:H films was observed to improve along with an increase of the optical gap. The spin density of *a*-SiO_x:H films was of the order of 10^{17} cm^{-9}. The optoelectronic properties of the films have been correlated with the bonding configurations in the film, deposition parameters and the growth kinetics.

1. Introduction

Insulating silicon dioxide (SiO_2) thin films are widely used as the gate oxide for thin film transistors (TFT) and as passivation layers in Very Large Scale Integration (VLSI) technology. Recently amorphous hydrogenated silicon oxide (*a*-SiO_x:H) has shown promise for use as a widegap semiconducting material in photovoltaic applications. Using *a*-SiO_x:H as the p-layer, single junction solar cells with an efficiency of 12.5% for a 1 cm^2 area have been reported [1]. In order to explore the possible application of *a*-SiO_x:H films in photovoltaic devices it is necessary to understand the growth process (or kinetics) and material properties as a function of deposition parameters and the method of film preparation. The majority of reports in the literature [1–4] on the preparation of *a*-SiO_x:H films consider the plasma chemical vapour decomposition (plasma-CVD) growth of films using a SiH_4, CO_2, H_2 and CO_2 (used as a source of oxygen) gas mixture. Unfortunately the plasma-CVD process is accompanied by a bombardment of the growing surface by energetic neutral and charged particles which causes damage to the substrate, interface and growing film. The photo-CVD method however does not suffer from the above disadvantages since the source gases are decomposed by either a UV light or a laser source. The CO_2 gas decomposes into CO and O (atomic oxygen) under irradiation by UV light [5] and thus oxygen is incorporated into the film during its growth. A careful examination of the infrared (IR) absorption spectra of the grown film confirms the absence of any contaminating carbon species.

Despite the above-mentioned advantages of the photo-CVD method very few reports exist in the literature on the preparation of *a*-SiO_x:H using the photo-CVD method [6, 7]. In this study, we attempt to optimize the deposition parameters for the development of high quality *a*-SiO_x:H films. An attempt is made to correlate the optoelectronic properties of these films with the deposition parameters and their growth kinetics. Finally, a comparison of the properties of the grown *a*-SiO_x:H films with conventional wide bandgap silicon carbide is presented.

2. Experimental procedures

The preparation of the amorphous hydrogenated silicon oxide films (*a*-SiO_x:H) was performed in a Hg-sensitized photo-CVD system (SAMCO, Japan). The gas mixtures of silane (SiH_4), carbon dioxide (CO_2) and hydrogen (H_2) were decomposed by the 185 and 254 nm wavelength UV light emitted from a low pressure mercury vapour lamp. A detailed description of the deposition system has been published elsewhere [8]. Hydrogen gas was introduced into the deposition chamber via a mercury pot which was maintained at 70 °C, thereby carrying mercury vapour into the reaction chamber. The substrate was maintained at a temperature of 250 °C while the UV light entered the chamber through a suprasil window. For each deposition, the chamber was degassed to a base vacuum better than 2.666×10^{-4} Pa with a turbomolecular pump, prior to the introduction of the source gases.

The films deposited onto 7059 Corning glass substrates for subsequent electrical and optical measurements were 300–500 nm thick. Films grown onto a *c*-Si wafer for IR and onto Al-foil for electron spin resonance studies were $\sim$1 μm thick, as measured by a Talystep. The reason for the large thickness of

0022–2461

the film for IR measurements was to avoid the previously reported thickness dependence of IR vibrational absorption [9]. The dark- and photoconductivity (under a 100 mW cm^{-2} white light illumination) of the samples annealed in vacuum at 150 °C for 1 h were measured in a gap cell geometry under a vacuum of 1.33×10^{-4} Pa. The refractive indices and the optical absorption values, corrected for surface reflection, were calculated from transmission spectra taken on a UV-VIS double beam spectrophotometer (Hitachi 330, Japan). Infrared (IR) vibrational spectra were obtained using a Fourier transform infrared (FTIR) spectrophotometer (Perkin Elmer 1700, UK) as the average of 100 scans obtained at a resolution of 4 cm^{-1}. The spin densities were calculated from electron spin resonance (ESR) spectra taken on powder samples at room temperature. The gas mixtures were characterized in terms of: Y, the ratio of the CO_2 to SiH_4 gas flows i.e., $Y = CO_2/SiH_4$ and Z the hydrogen dilution given by $Z = H_2/(CO_2 + SiH_4)$.

3. Results

3.1. The effect of varying the oxygen concentration

3.1.1. Optical and electrical properties

Hydrogenated amorphous silicon oxide films (a-SiO_x:H) were grown at a constant hydrogen flow while Y was varied from 0 to 10.2. The chamber pressure was maintained at 1.333×10^2 Pa using a throttle valve. The optical bandgap of the films, E_g, was estimated following the method of Davis and Mott [10] by extrapolating the linear section observed in the high absorption region ($\alpha > 10^4$ cm^{-1}) of a $(\alpha h\nu)^{1/2}$ versus $h\nu$ plot to $\alpha = 0$ where α is the absorption coefficient and $h\nu$ is the proton energy. The refractive index (n_f) was measured from the fringe pattern of the transmission spectra in the near infrared (NIR) region. Fig. 1 depicts the variations of the optical gap (E_g), refractive index (n_f), photoconductivity (σ_{ph}), dark conductivity (σ_d) and its activation energy (E_a), as a function of the CO_2 to SiH_4 gas flow ratio. The optical gap increases monotonically from 1.8 to 2.44 eV with an increase in the molar fraction ratio of CO_2 to SiH_4 and hence the oxygen content in the film. The refractive index n_f decreases consistently from 3.2 to 1.92 with Y. Both the dark- and photoconductivity values decrease with Y but the dark conductivity activation energy, E_a, increases showing an inverted replica of the σ_d curve. Similar trends have been previously reported [11] but in our case, the photoconductivity values are somewhat superior. The observed deterioration in the photoconductivity value with increasing Y is accompanied by a shift of the dark condition Fermi level as revealed by the activation energies of the dark conductivities. Considering that the transport is mainly due to electrons, one may conclude that as the amount of oxygen incorporation increases, the optical gap expands and the dark Fermi level is shifted to the mid-gap. The samples exhibit photosensitivity, defined as the ratio of σ_{ph} to σ_d, in the range of 10^6 to 10^7. It should be noted that the film prepared with a Y value of 1.4 displays a white light photoconductivity value of 1.4×10^{-4} S cm^{-1} and an E_g of 1.89 eV. Such a high photoconductivity value has not been previously reported for either a-SiC:H or a-SiO_x:H films.

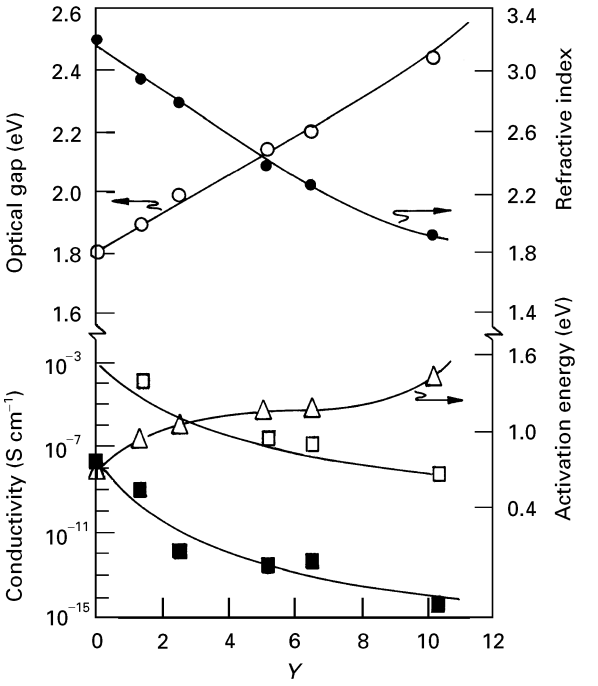

Figure 1 (○) Optical gap E_g, (●) refractive index n_f, (□) photoconductivity σ_{ph}, (■) dark conductivity σ_d and (△) its activation energy E_a as function of molar fraction of CO_2 to SiH_4 in the gas phase (Y).

3.1.2. Bonding configuration

In a multicomponent material, the mixing of the constituent atoms is expected to affect the optoelectronic properties of the films. The mixing of the constituent atoms is generally investigated by means of photoelectron spectroscopy. However this method requires sputter-etching (in order to avoid any surface contamination) which often changes the structure near the film surface. To overcome this problem IR absorption measurements have been performed and the data analysed to gain an insight into the bonding configurations and the mixing of the constituent atoms. The IR absorption spectra measured in the range 900–1250 cm^{-1} for four different films prepared with Y values of 1.4, 2.6, 6.5, and 10.2 are shown in Fig. 2. According to the random-bonding model (RBM) [12], a-SiO_x (with $x < 2$) films are composed of five basic $Si–O_n–Si_{4-n}$ ($n = 0$–4) bonding configurations with four of them ($n = 1$–4) being IR active. The basic configurations along with bonding unit and peak position of the SiO stretching absorption ($\nu_{SiO}(n)$) are presented in Table 1. The positions of the basic configurations are also indicated on the curves of Fig. 2. The curves may be deconvoluated into Gaussian profiles about the assigned peaks. It is clear that with an increase in the value of the deposition parameter Y, there is an increase in the oxygen content in the bonding unit. In other words, oxygen becomes incorporated into the film with an increase in the value of Y. It can be seen from Fig. 2 that with an increase in the

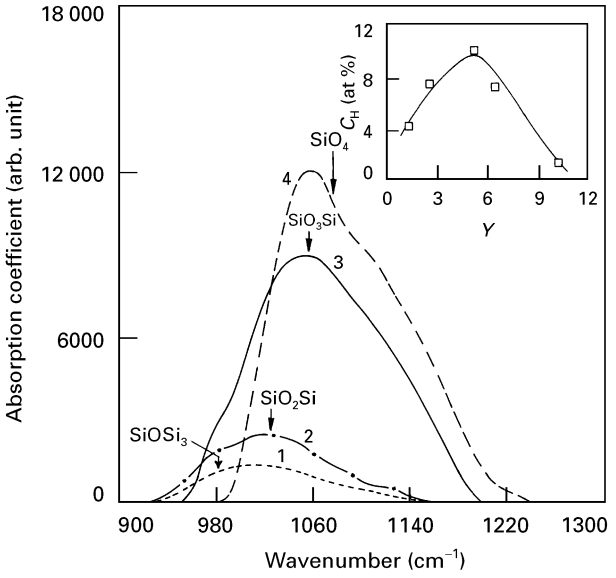

Figure 2 The IR absorption spectra, in the Si–O stretching region of a-SiO_x:H films prepared at different CO_2 to SiH_4 ratios (Y): (1) $Y = 1.4$, (2) $Y = 2.6$, (3) $Y = 6.5$ and (4) $Y = 10.2$. The inset represents the hydrogen content C_H (in at %) as a function of Y.

TABLE I Basic configurations and bonding units on the basis of the RBM of a-SiO_x. $\nu_{SiO}(n)$ is the calculated peak frequency of the SiO stretching absorption [25]

n	Basic configuration	Bonding unit	($\nu_{SiO}(n)$) (cm^{-1})
1	Si–O–Si_3	Si_3O	980
2	Si–O_2–Si_2	SiO	1025
3	Si–O_3–Si	Si_2O_4	1055
4	SiO_4	SiO_2	1076

value of Y the area under the curve increases and the peak shifts to higher wavenumbers. The oxygen related bridging bond (Si–O–Si) centred around 1000 cm^{-1} gradually shifts [13] towards higher wavenumbers and for a Y value of 10.2 a shoulder at $\sim$1120 cm^{-1} can be observed. The shift of peak position (w_0^5) with oxygen content i.e., an empirical linear relation of w_0^5 with oxygen content was verified by Pai *et al.* [14]. The bonded hydrogen content (C_H), in atomic per cent, was evaluated from the integrated stretching absorption peak area around 2000 cm^{-1}. It should be noted that the accuracy of this method is limited by possible variations in the oscillator strength with the oxygen content in the films. It is interesting to observe from the inset of Fig. 2 that the hydrogen content (C_H) initially increases and then decreases as Y increases. However the integrated absorption area of the SiO band is found to gradually increase with Y.

3.1.3. Spin density

Table II summarizes the spin defect density, N_S, and g-values along with the optical gap and photoconductivity values for films at two different Y values. The spin density increases from 2.6×10^{17} to 3.4×10^{17} with an increase of Y from 2.6 to 10.2. The spin g value, estimated by using an Mn^{2+} marker, is found to decrease with Y. These results are similar to those previous reported in the literature [15, 16].

3.2. Effect of chamber pressure

The chamber pressure plays a significant role in changing the quality of a film produced by the photo-CVD process. Thus in order to optimize the film properties films were grown at different chamber pressures keeping Y and Z fixed at 2.7 and 1.1 respectively. The variation of optical gap (E_g), refractive index (n_f), photoconductivity (σ_{ph}) and dark conductivity (σ_d) as a function of the total chamber pressure (p_t) are shown in Fig. 3. One can see that E_g systematically decreases with an increase of p_t whereas n_f increases. The increase in the n_f value at higher p_t values is an indication of a compact structure containing few voids. Both the conductivities bear a positive correlation. Evidently the film grown at a p_t value of 1.333×10^2 Pa exhibits an impressive photoconductivity of 1×10^{-6} S cm^{-1} at a reasonably high E_g value of 1.99 eV. At 1.995×10^2 Pa a photoconductivity value of 2.33×10^{-5} S cm^{-1} with a band gap of 1.93 eV is observed.

Fig. 4 shows the IR absorption profiles of the SiH stretching mode in the range 1950–2350 cm^{-1} for films deposited at p_t values of 6.65×10^1, 1.33×10^2 and 1.995×10^2 Pa. The Si–O stretching modes of these samples are indicated in the inset of Fig. 4. It can be seen that IR absorption related to the Si–O stretching mode decreases and the peak shifts towards lower wavenumbers with an increase in p_t, which indicates relatively less Si–O bonding occurs at higher chamber pressure. It has been suggested that in a-SiO_x:H films, oxygen and hydrogen are bonded to the same Si atoms in the configuration H–Si ($Si_{3-n}O_n$) for $n = 1$–3, with peaks appearing at 2115, 2200 and 2260 cm^{-1} for $n = 1, 2, 3$, respectively. Curve 1 exhibits all the above three absorption peaks while the remaining curves show smaller absorptions at 2200 and 2260 cm^{-1}. A feature of particular importance in all the curves is the appearance of a shoulder at 2020 cm^{-1} for a p_t value of 1.995×10^2 Pa. This peak is the SiH stretching peak normally at 2000 cm^{-1} that has been shifted due to the presence of the oxygen.

TABLE II Optical gap, photoconductivity, dangling bond density and g value for a-SiO_x:H films prepared under different conditions

Y	Optical gap E_g (eV)	Photoconductivity σ_{ph} (S cm^{-1})	Dangling bond density $N_S \times 10^{17}$(cm^{-3})	g
2.6	1.99	9.66×10^{-7}	2.6	2.005 15
10.2	2.44	5.12×10^{-9}	3.4	2.004 78

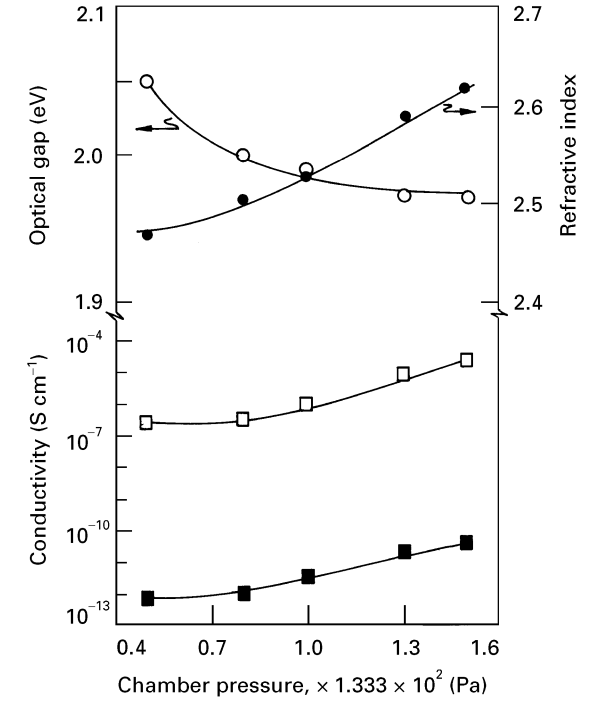

Figure 3 Dependence of: (○) optical gap E_g, (●) refractive index n_f, (■) dark conductivity σ_d and (□) photoconductivity σ_{ph} on the total chamber pressure.

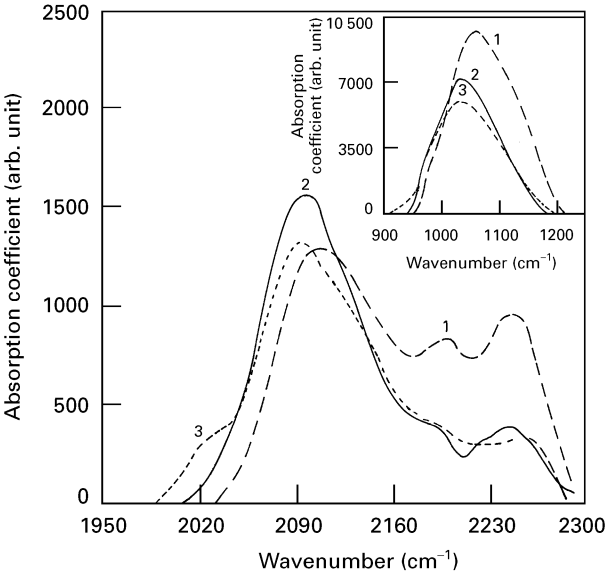

Figure 4 IR vibrational spectra over the wavenumber range 1950–2300 cm^{-1} for a-SiO_x:H films grown at different chamber pressures: (1) 6.65×10^1 Pa, (2) 1.33×10^2 Pa, (3) 1.995×10^2 Pa. The inset represents the Si–O stretching region for the same films.

3.3. Effect of hydrogen dilution

In order to gain an insight into the effect of hydrogen dilution (Z), defined in the experimental section, on the properties of the samples, the films were deposited under various hydrogen dilutions, with a constant CO_2 to SiH_4 flow ratio (Y) of 2.6. The properties and the deposition rates of the a-SiO_x:H films grown at different hydrogen dilutions are summarized in Table III. It can be seen from this table that E_g increases monotonically with increasing Z values which is in contrast to the case of a-SiC:films where E_g decreases with an increase in the hydrogen dilution [17]. The photoconductivity of the films improves from 2.89×10^{-7} to 1.06×10^{-6} S cm^{-1} when the hydrogen dilution is increased from 0.28 to 2.2 although the band gap (E_g) increases from 1.96 to 2.06 eV. The photosensitivity of the sample is 10^6 when prepared with a high hydrogen dilution.

3.4. Comparison of the properties of a-SiO_x:H with that of a-SiC_x:H

As a wide bandgap material amorphous silicon carbide finds application in a-Si solar cells. In a-SiC_x:H films unbonded carbon contamination can be high. This problem can be circumvented by a higher hydrogen dilution which encourages bond formation between hydrogen and carbon. A comparison of the optoelectronic properties of the grown a-SiO_x:H films (curve 1) with that of a-SiC_x:H (curves 2 and 3) is shown in Fig. 5. The films represented by curve 2 were deposited without any hydrogen dilution whilst those represented by curve 3 were deposited under a hydrogen dilution ratio of 10 [18]). The room temperature photoconductivity of an a-SiO_x:H film has been measured with a photon flux of 10^{15} cm^{-2} s^{-1} and a photo energy of 2.38 eV. Fig. 5 shows the variation in photoconductivity for two materials – a-SiC_x:H and a-SiO_x:H; with optical gap. It can be seen that for optical gaps upto 2.0 eV both materials show the same photoconductivity but at higher optical gaps the photoconductivity of the oxide sample is higher than that of the carbide sample. It has been observed [16, 18] that the increase in the optical gap is greater for a-SiO_x:H than for a-SiC_x:H for the same increase in x (anion content). This could be due to the fact that the bond strength of Si–O is stronger than that of Si–C. The incorporation of oxygen or carbon leads to an increase in the density of defects, depending on the

TABLE III Variation of optical gap E_g, photoconductivity σ_{ph}, dark conductivity σ_d and the integrated absorption intensity of SiO stretching mode I^S_{SiO} with hydrogen dilution

Z	Optical gap E_g (eV)	Dark conductivity $\sigma_d \times 10^{-12}$ (S cm^{-1})	Photoconductivity $\sigma_{ph} \times 10^{-7}$ (S cm^{-1})	Integrated intensity I^5_{SiO} (cm^{-2})
0.28	1.96	4.48	2.89	—
0.56	1.97	8.21	3.61	—
0.84	1.98	0.376	2.77	200
1.12	1.99	1.31	9.66	292
2.24	2.08	0.973	1.01	719

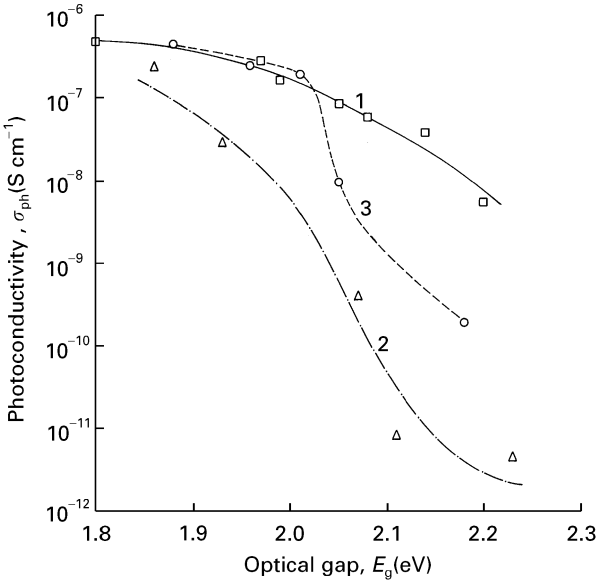

Figure 5 Variation of the photoconductivity (under a photon flux of 10^{15} cm^{-2} S^{-1}) with the optical gap for (□) curve 1 *a*-SiO_x : H, (△) curve 2 *a*-SiC : H prepared without H_2 dilution and (○) curve 3 *a*-SiC : H prepared with H_2 dilution.

amount of incorporation. For effective utilization of solar radiation, the optical gap of the window layer of the solar cell should be around 2.0 eV.

4. Discussion

In the mercury sensitized photo-CVD process, fragments of the gaseous molecules (SiH_4, CO_2 and H_2) are produced by the excited Hg atoms. The gases are photo-dissociated, resulting in many new species and radicals [5, 19] such as:

$$SiH_4 + Hg^* \rightarrow SiH_3 + H + Hg \quad (1)$$

or

$$SiH_2 + 2H + Hg \quad (2)$$

$$CO_2 + Hg^* \rightarrow CO + O + Hg \quad (3)$$

$$H_2 + Hg^* \rightarrow 2H + Hg \quad (4)$$

It has been reported that the oxygen content in *a*-SiO_x : H films has an almost linear relationship with the CO_2 to SiH_4 gas flow ratio. Thus a positive correlation between the optical gap and the molar fraction of CO_2 to SiH_4 is surely due to the incorporation of more oxygen into the film. This in turn is due to the point that the Si–O bond is stronger than an Si–Si bond due to the high electronegativity of oxygen. The increase in the optical gap is accompanied by a decrease in the value of the refractive index which gives a qualitative idea about the film composition. The decrease of the refractive index may be reasoned to be due to an increase in the number of voids, microstructural defects and disorder in the film following the incorporation of the oxygen. In fact, the oxygen incorporation results in an increase in the structural and electronic disorder as a result of the difference in the bond length between 0–0 (0.146 nm) and Si–Si (0.235 nm). Recently, experimental evidence showing an increase in the spin defect densities with increasing oxygen content [2, 16] was found for this hypothesis. Thus the observed deterioration in the photoconductivity with incorporation of oxygen may be due to an increase in the electronic and structural disorders and also the spin defect density in the film. An apparent disagreement between the observed peak position of the SiO stretching absorption curve and the indicated peak position of the bonding configuration is attributed to the aggregated effect of the component absorptions when the curves are properly deconvoluted. It has been suggested in the literature that the observed shift of the SiO stretching mode peak is the direct consequence of the increased oxygen content in the film [14, 20]. This increase in the oxygen content with CO_2 molar fraction in the cause of the enhancement of the spin density and hence the decrease in the photoconductivity value. Moreover the g value decreases with increasing oxygen content in the film. The variation of C_H can be correlated with the increase in SiO bonds produced by an increase of Y by the following argument. At low concentrations of oxygen in the reaction chamber the Si sites may be taken up by either oxygen or hydrogen. Initially as Y increases, then the SiO content increases. As the partial pressure of hydrogen decreases, the hydrogen coverage of the surface decreases and more SiH bonds are formed. With a further increase in Y ($Y > 5.2$), the number of Si–O bonds increases, however the deficiency of H atoms means that the density of Si–H bonds continues to decrease.

When the chamber pressure is increased while the gas flow ratio is kept constant, the residence times of the gas molecules increases. This facilitates the fragmentation of molecules and that of SiH_4 will be greater than that of CO_2 because of the higher quenching cross-section of the former [21]. Moreover, Saxena *et al.* [22] have shown, by a model gas phase calculation that the increase in the flux of SiH_3 and SiH_2 radicals at the growth surface increases with an increase in the chamber pressure. Thus it may be concluded that with an increase of pressure the film becomes oxygen deficient. This accounts for the observed decrease in the optical gap with chamber pressure. The observed decrease in SiO absorption intensity in conjunction with the shift of the peak towards lower wavenumbers is also a signature of the decrease of oxygen content in the film with an increase of the chamber pressure. The improvement in photoconductivity with chamber pressure is evidently due to a decrease in the oxygen content and a consequent better structural ordering with less voids and defects. One may assume that the films prepared at high pressures are Si-rich while those at lower pressures are oxygen rich. It has been proposed [23] that the silicon oxide films may be thought of as a mixture of two structures: the oxygen-rich phase is effective in increasing the optical gap while the photo-generated carriers mainly travel through the silicon-rich phase.

An increase in hydrogen dilution leads to the creation of more atomic hydrogen which is believed to cover the growing surface. Thus the decrease of film growth rate with hydrogen dilution is clearly due to

depletion of precursors namely SiH_3 and SiH_2 and hydrogen coverage. Unlike *a*-SiC : H, the most striking result for *a*-SiO_x : H is the increase in the optical gap with hydrogen dilution. The enhancement of the optical gap is corroborated by the increase in the integrated SiO peak area and hence the incorporation of oxygen. With the increase of hydrogen dilution, gas phase secondary reactions are expected. As a result, the dominant film growing precursor SiH_3 is removed from the reaction by combining with atomic hydrogen. This paves the way for atomic oxygen to be incorporated into the film due to the relatively low SiH_3 flux at the growth surface with hydrogen dilution. The increase in the spin density from 2.68×10^{17} to 3.75×10^{17} due to an increase in the hydrogen dilution (Z) from 1.12 to 2.24 is an endorsement of the increase in oxygen content. The improvement in the photo-current with hydrogen dilution can be attributed to a better relaxation of the network of the film produced by a decrease in the growth rate. Moreover, with an increase in the hydrogen dilution, the hydrogen coverage of the growth surface enables energy relaxation of the absorbed precursors [24] leading to a denser network structure and hence improved optoelectronic properties.

5. Conclusions

Amorphous silicon oxide films have been prepared by photo chemical vapour decomposition of a SiH_4, CO_2 and H_2 gas mixture. The optical gap was found to increase with an increase in the CO_2 to SiH_4 flow ratio i.e., with the incorporation of oxygen. The optoelectronic and structural properties of the films are sensitive to the chamber pressure. At higher pressures the formation of lower order oxides predominates. An increase in the hydrogen dilution increases the oxygen incorporation into the films and as a consequence the band gap increases. A decrease in the photoconductivity and refractive index and a simultaneous increase in the spin density with oxygen incorporation have been attributed to an increase of structural and electronic disorder. Finally *a*-SiO_x : H films have better optoelectronic properties compared to *a*-SiC_x : H at $E_g > 2.0$ eV.

Acknowledgement

This work has been carried out under a project funded by the ministry of Non-Conventional Energy Sources, Government of India.

References

1. Y. ICHIKAWA, S. FUJIKAKE, H. OHTA, T. SASAKI and H. SAKAI, in Proceedings of the 22nd IEEE Photovoltaic Conference, Las Vegas, 1991 (IEEE Electron Devices Society) p. 1296.
2. A. MORIMOTO, H. NORIYAMA and T. SHIMIZU, *Jpn J. Appl. Phys.* **26** (1987) 22.
3. M. LIEHR and S. A. COHEN, *Appl. Phys. Lett.* **60** (1992) 198.
4. A. SINGH and E. A. DAVIS, *J. Non-Cryst. Solids* **122** (1990) 223.
5. H. OKABE, "Photochemistry of small molecules" (Wiley, New York, 1978) p. 145.
6. Y. TARUI, J. HIDAKA and K. AOTO, *Jpn J. Appl. Phys.* **23** (1984) L827.
7. P. GONJALEZ, D. FERNANDEZ, J. POU, E. GARCIA, J. SERRA, B. LEON and M. PEREZ-AMOR, *Thin Solid Films* **218** (1992) 170.
8. S. GHOSH, A. DASGUPTA and S. RAY, *J. Appl. Phys.* **78** (1995) 3200.
9. A. A. LONGFORD, M. L. FLEET, B. P. NELSON, W. A. LANFORD and N. MALEY, *Phys. Rev.* **B45** (1992) 13 367.
10. E. A. DAVIS and N. F. MOTT, *Phil. Mag.* **22** (1970) 903.
11. K. HAGA, K. YAMAMOTO, M. KUMANO and H. WATANABE, *Jpn J. Appl. Phys.* **25** (1986) L39.
12. H. R. PHILIPP, *J. Non-Cryst. Solids* **8–10** (1972) 627.
13. E. C. FREEMAN and W. PAUL, *Phys. Rev.* **B18** (1978) 4288.
14. P. G. PAI, S. S. CHAO, Y. TAKAGI and G. LUCOVSKY, *J. Vac. Sci. Technol.* **A4** (1986) 689.
15. E. HOLZENKAMPFER, F. W. RICHTER, J. STUKE and U. VOGET-GROTE, *J. Non-Cryst. Solids* **32** (1979) 327.
16. S. OTSUBO, M. SAITO, A. MORIMOTO, M. KUMEDA and T. SHIMIJU, *Jpn J. Appl. Phys.* **27** (1988) 1999.
17. A. MATSUDA, T. YAMAOKA, S. WOLFF, M. KOYAMA, Y. IMANISHI, H. KATAOKAM, H. MATSUURA and T. TANAKA, *J. Appl. Phys.* **60** (1986) 4025.
18. S. H. BAKER, W. E. SPEAR and R. A. G. GIBSON, *Phil. Mag.* **B62** (1990) 213.
19. E. KAMARATONS and F. W. LAMPE, *J. Phys. Chem.* **74** (1970) 2267.
20. G. LUCOVSKY, C. K. WONG and W. B. POLLARD, *J. Non-Cryst. Solids* **59–60** (1983) 839.
21. M. KONAGAI, *Mater. Res. Soc. Symp. Proc.* **70** (1986) 257.
22. N. SAXENA, C. M. FORTMANN and T. W. F. RUSSELL, *ibid* **149** (1989) 99.
23. H. WATANABE, K. HAGA and T. LOHNER, *J. Non-Cryst. Solids* **164–166** (1993) 213.
24. A. MATSUDA and K. TANAKA, *ibid* **97–98** (1987) 1367.
25. L. HE, T. INOKUMA, Y. KURATA and S. HASEGAWA, *ibid* **185** (1995) 249.

Received 25 March 1996
and accepted 21 March 1997